J|A|C|S
ARTICLES
Published on Web 12/30/2004

Reactivity of Peroxo Forms of the Vanadium Haloperoxidase Cofactor. A DFT Investigation

Giuseppe Zampella,† Piercarlo Fantucci,† Vincent L. Pecoraro,*,‡ and Luca De Gioia*,†

Contribution from the Department of Biotechnology and Biosciences, University of Milano-Bicocca, Piazza della Scienza 2, 20126 Milano, Italy and Department of Chemistry, University of Michigan, Ann Arbor, Michigan, 48109-1055

Received July 5, 2004; Revised Manuscript Received November 2, 2004; E-mail: vlpec@umich.edu; luca.degioia@unimib.it

Abstract: Density functional theory has been used to investigate structural, electronic and reactivity properties of complexes related to the peroxo forms of vanadium haloperoxidases (VHPO). In particular, the reactivity of the cofactor as a function of protonation state and environment, which are two factors thought to be crucial in modulating the activity of the enzyme, has been examined. In full agreement with experimental data, results highlight the role of protonation in the activation of the peroxo-vanadium complexes and show that the oxo-transfer step involves the unprotonated axial peroxo oxygen atom, which is easily accessible to substrates in the peroxo form of the enzyme. The role of Lys353, which in the X-ray structure of the peroxide-bound form of vanadium chloroperoxidase is hydrogen bonded to the equatorial oxygen atom of the peroxo group, has been also explored. It is concluded that Lys353 can play a role similar to a H^+ in the activation of the peroxo form of the cofactor.

Introduction

Vanadium haloperoxidases (VHPOs) are enzymes that catalyze the oxidation of halide ions by hydrogen peroxide to the corresponding hypohalous acids and are capable of halogenating organic substrates[1]

$$H_2O_2 + H^+ + X^- \rightarrow H_2O + HOX$$

Each enzyme is named based on its ability to oxidize halides with chloroperoxidases capable of oxidizing chloride, bromide, and iodide while bromoperoxidases are unable to oxidize chloride. A variety of organic substrates can be halogenated and dimerized while thioethers oxygenated to sulfoxides.

Insight into the structural features of the inorganic cofactor and its environment were obtained by X-ray diffraction of the VClPO from the pathogenic fungus *Curvularia inaequalis*.[2,3] In the native state,[2] the vanadium ion is characterized by a trigonal bipyramidal geometry, where three oxygen atoms belong to the equatorial plane and one oxygen occupies an axial position. The other apical ligand is His496, which links the metal ion to the protein, whereas Lys353, Arg360, His404, and Arg490 are involved in hydrogen bonds with the oxygen atoms of the cofactor. In the peroxo derivative of the enzyme,[3] the cofactor is characterized by a strongly distorted trigonal bipyramidal geometry, with two oxo type oxygen atoms and one peroxo atom in the equatorial plane, while His496 and the other peroxo atom occupy axial positions (Figure 1). Crystallographic analysis of other VHPOs have shown that the first and second coordination sphere of the cofactor is well conserved across species.[4,5]

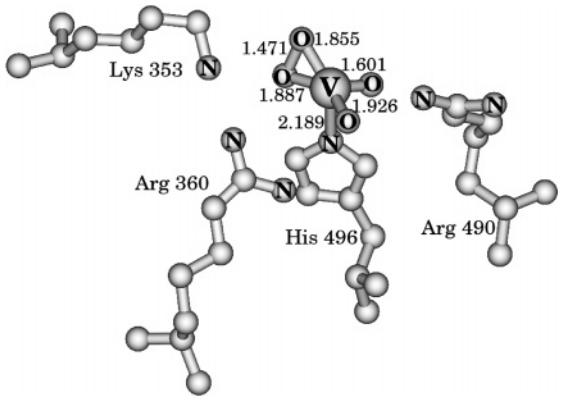

Figure 1. Structure of the peroxo form of the active site of the vanadium containing haloperoxidase from the fungus *Curvularia inaequalis*, as obtained by X-ray diffraction.[3] Relevant distances in Å.

The catalytic properties of VHPOs have been extensively investigated in recent years,[1] leading to the conclusion that vanadium remains in the V(V) oxidation state throughout the catalytic cycle. The role of the metal is to serve as a strong

† University of Milano-Bicocca.
‡ University of Michigan.

(1) de Boer, E.; Wever, R. *J. Biol. Chem.* **1988**, *263*, 12326−12332; Van Schijndel, J. W. P. M.; Barnet, P.; Roelse, J.; Vollenbroek, E. G. M.; Wever, R. *Eur. J. Biochem.* **1994**, *225*, 151−157; Everett, R. R.; Soedjak, H. S.; Butler, A. *J. Biol. Chem.* **1990**, *265*, 15671−15679; Butler, A. *Coord. Chem. Rev.* **1999**, *187*, 17−35.
(2) Messerschmidt, A.; Wever, R. *Proc. Natl. Acad. Sci. U.S.A.* **1996**, *93*, 392−396.
(3) Messerschmidt, A.; Prade, L.; Wever, R. *Biol. Chem.* **1997**, *378*, 309−315.
(4) Weyand, M.; Hecht, H.-J.; Kie, M.; Liaud, M.-F.; Vilter, H.; Schomburg, D. *J. Mol. Biol.* **1999**, *293*, 596−611.
(5) Isupov, M. N.; Dalby, A. R.; Brindley, A. A.; Izumi, Y.; Tanabe, T.; Murshudov, G. N.; Littlechild, J. A. *J. Mol. Biol.* **2000**, *299*, 1035−1049.

Lewis acid in the activation of the primary oxidant H_2O_2. It has been observed that Lys353, which is the only amino acid interacting directly with the peroxo-bound moiety, might polarize the peroxo bond, making it more susceptible toward nucleophilic attack. In fact, mutagenesis experiment showed that a large decrease in activity is observed for the K353A mutant.[6] Experimental studies indicate also that the hypohalous acid formed can work as a site-selective halogenating agent as it is,[7,8] or, especially in case of bromide and iodide, as X_3^-.[1]

The investigation of synthetic peroxo-vanadium complexes has been particularly relevant for understanding the reactivity of this class of compounds. Several have been shown to be good functional models of VHPO.[9−20] The rate of halide oxidation is generally increased by addition of acids and spectroscopic data are consistent with the protonation of one or more sites on the complex, suggesting that the heterolytic cleavage of the peroxide O−O bond could be assisted by generation of a side-on bound hydroperoxide.[9,21] However, the synthesis of models characterized by the metal coordination environment observed in the enzyme has not yet been achieved,[22] hindering direct comparison with the chemical properties of the cofactor within the enzyme active site. Specifically, it is not known whether the protonation of the peroxo group is a prerequisite for activation in the enzyme and, if so, whether the protonated or unprotonated oxygen atom is the site of halide attack. Moreover, other relevant issues remain unsolved. The X-ray structure of the peroxo derivative of VHPO reveals a potentially vacant coordination site, leading to the observation that halide might bind to vanadium prior to oxidation.[23] Finally, it is not known whether the oxo-transfer involves the equatorial or the pseudo-axial peroxo oxygen atom.

Quantum chemical methods can be useful tools to investigate structural, electronic and reactivity properties of transition metal complexes[24] and models of the active site of metallo-enzymes.[25] In fact, some computational investigations of vanadium (V) complexes have been reported,[13,26−28] even though theoretical models characterized by the metal coordination environment observed in VHPOs have only recently been studied.[29]

In this contribution, we have used density functional theory (DFT) to investigate structural, electronic, and reactivity properties of complexes related to the peroxo forms of VHPO as a function of environment and protonation state. In the first section of the paper, we present the characterization of the peroxo cofactor as a function of protonation state. Then, the reactions of anionic (Br^-) and neutral (dimethyl sulfide) substrates with the most stable peroxo forms of the cofactor have been investigated. In the last section, we present results for the oxo-transfer step in models characterized by essential features of the cofactor, as observed within the enzyme. Results highlight the role of protonation in the activation of peroxo-vanadium complexes, in agreement with experimental data,[6,9,30] and show that the oxo-transfer step involves the unprotonated axial peroxo oxygen atom, which is easily accessible to substrates in the peroxo form of the enzyme.[3] Results indicate also that the lysine residue (K353) that is hydrogen bonded to the equatorial peroxo atom in the enzyme[3,30] can play a role similar to H^+ in the activation of the peroxo form of the cofactor. This observation may help in driving the design of new functional model complexes.[30]

Methods

DFT structure optimizations were carried out using the BP86 functional[31] and an all-electron valence triple-ζ basis set with polarization functions on all atoms (TZVP).[32] Calculations have been carried out using the Turbomole suite of programs[33] in connection with the resolution of the identity technique.[34,35]

The optimization of the transition state structures has been carried out according to a procedure based on a pseudo Newton−Raphson method. Initially, geometry optimization of a guessed transition state structure is carried out constraining the distances corresponding to the reaction coordinate, namely the peroxo O−O and the X−O (where X is either Br^-, Cl^- or the sulfur atom of dimethyl sulfide) interatomic distances. The initial Hessian matrix for such optimization is calculated at the classical level, whereas the BP86-RI/TZVP level is used to compute the Hessian matrix of the minimum energy structure. Vibrational analysis of the minimum energy structures is carried out and, if one negative eigenmode corresponding to the reaction coordinate exists, the curvature determined at such point is used as starting point in the transition state search. The location of the transition state structure is carried out using an eigenvector-following search: the eigenvectors in the Hessian are sorted in ascending order, the first one being that associated to the negative eigenvalue. After the first step, however, the search is performed by choosing the critical eigenvector with a maximum overlap criterion, which is based on the dot product with the eigenvector followed at the previous step.

The optimized structures of the transition states are labeled as follow: the first character indicates the protonation state of the cofactor

(6) Hemrika, W.; Renirie, R.; Macedo-Ribeiro, S.; Messerschmidt, A.; Wever, R. *J. Biol. Chem.* **1999**, *274*, 23820−23827.
(7) Clague, M. J.; Keder, N. L.; Butler, A. *Inorg. Chem*. **1993**, *32*, 4754−4761.
(8) Martinez, J. S.; Carrol, G. L.; Tschirret-Guth, R. A.; Altenhoff, G.; Little, R. D.; Butler, A. *J. Am. Chem. Soc.* **2001**, *123*, 3289−3294.
(9) Colpas, G. J.; Hamstra, B. J.; Kampf, J. W.; Pecoraro, V. L. *J. Am. Chem. Soc.* **1996**, *118*, 3469−3478.
(10) Slebodnick, C.; Hamstra, B. J.; Pecoraro, V. L. In *Metal Sites in Proteins and Models*; Sandler, P. J., Ed.; Springer-Verlag: Berlin, 1997, Vol. 89, pp 51−108.
(11) (a) Rehder, D. *Inorganic Chemistry Communications* **2003**, *6*, 604−617; (b) Rehder, D. *Coord. Chem. Rev.* **1999**, *182*, 297−322.
(12) Buhl, M.; Schurhammer, R.; Imhof, P. *J. Am. Chem. Soc.* **2004**, *126* (10), 3310−3320.
(13) Conte, V.; Bartolini, O.; Carraro, M.; Moro, S. *J. Inorg. Biochem.* **2000**, *80*, 41−49.
(14) Mimoun, H.; Saussine, L.; Daire, E.; Postel, M.; Fischer, J.; Weiss, R. *J. Am. Chem. Soc.* **1983**, *105*, 3101.
(15) Butler, A.; Clague, M. J.; Meister, G. E. *Chem. Rev.* **1994**, *94*, 625−638.
(16) Bortolini, O.; Di Furia, F.; Scrimin, P.; Modena, G. *Nouv. J. Chim*. **1985**, *9*, 147.
(17) Ballistreri, F. P.; Tomasselli, G. A.; Toscano, R. M.; Conte, V.; Di Furia, F. *J. Am. Chem. Soc.* **1991**, *113*, 6209.
(18) Smith, T. S., II.; Pecoraro, V. L. *Inorg. Chem*. **2002**, *41*, 6754−6760.
(19) Plass, W. *Coord. Chem. Rev.* **2003**, *237*, 205−212.
(20) Ligtenbarg, A. G. J.; Hage, R.; Feringa, B. L. *Coord. Chem. Rev.* **2003**, *237*, 89−101.
(21) Casny, M.; Rehder, D.; Schmidt, H.; Vilter, H.; Conte, V. *J. Inorg. Biochem.* **2000**, *80*, 157−160.
(22) Ligtenbarg, A. G. J. "*Vanadium and Iron Complexes for Catalytic Oxidation*", Ph.D. Thesis, 2001.
(23) Messerschmidt, A.; Wever, R. *Inorg. Chim. Acta* **1998**, 160−166.
(24) Niu, S.; Hall, M. B. *Chem. Rev.* **2000**, *100*, 353−405.
(25) Siegbahn, P. E. M.; Blomberg, M. R. A. *Chem. Rev.* **2000**, *100*, 421−437.
(26) Buhl, M. *J. Comput. Chem.* **1999**, *20*, 1254−1261.
(27) Conte, V.; Difuria, F.; Moro, S.; Rabbolini, S. *J. Mol. Catal. A Chem.* **1996**, *113*, 175−184.
(28) Balcells, D.; Maseras, F.; Lledos, A. *J. Org. Chem.* **2003**, *68*, 4265−4274.
(29) Zampella, G.; Yudenfreund Kravitz, J.; Webster, C. E.; Fantucci, P.; Hall, M. B.; Carlson, H. A.; Pecoraro, V. L.; De Gioia, L. *Inorg. Chem.* **2004**, *43*, 4127−4136.
(30) Kimblin, C.; Bu, X.; Butler, A. *Inorg. Chem.* **2002**, *41*, 161−163.
(31) Becke, A. D. *Phys. Rev. A* **1988**, *38*, 3098; Perdew, J. P. *Phys. Rev. B* **1986**, *33*, 8822.
(32) Schafer, A.; Huber, C.; Ahlrichs, R. *J. Chem. Phys.* **1994**, *100*, 5829.
(33) Ahlrichs, R.; Bar, M.; Haser, M.; Horn, C.; Kolmel, C. *Chem. Phys. Lett.* **1989**, *162*, 165.
(34) Eichkorn, K.; Treutler, O.; Öhm, H.; Haser, M.; Ahlrichs, R. *Chem. Phys. Lett.* **1995**, *240*, 283.
(35) Eichkorn, K.; Weigend, F.; Treutler, O.; Ahlrichs, R. *Theor. Chem. Acc.* **1997**, *97*, 119.

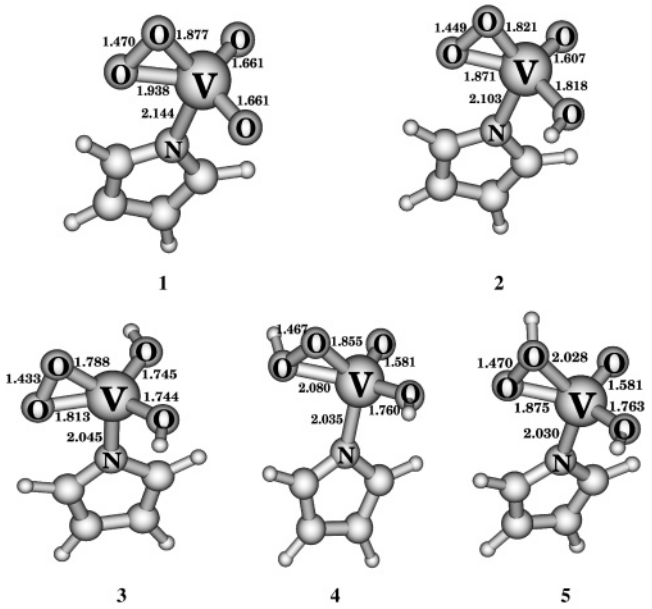

Figure 2. Optimized structures of the model complexes **1**, **2**, **3**, **4**, and **5**. Distances in Å.

according to the nomenclature adopted for the model complexes; the second part defines the substrate of the reaction (either dimethyl sulfide or bromide), whereas the third is related to the reacting peroxo oxygen atom ('a' stands for axial, 'e' for equatorial).

Full vibrational analysis has been carried out to characterize each stationary point. Potential energy barriers have been calculated using as reference the energy of the optimized reactant adducts. Partial atomic charges have been computed according to the Natural Atomic Orbital scheme.[36]

The effect of the protein environment has been evaluated with the solvent continuous model approach COSMO[37] as implemented in the Turbomole package. Even if this is a quite crude way to describe the protein matrix interacting with the cofactor, the polarizable continuum medium is expected to mimic simply the presence of amino acids surrounding the metal cofactor in VHPO. To this purpose, the dielectric constant ϵ was set to 40, a value that has been suggested to take into account the effect of charge−charge interactions in proteins.[37,38] To better address specific issues (see below) the cofactor environment has been described using explicit amino acid models and counterions.

Results and Discussion

Protonated Forms of the Peroxo Vanadium Cofactor. DFT optimization of the anionic peroxo form of the cofactor $[ImVO_4]^-$ leads to **1**, in which the vanadium coordination environment can be described as a strongly distorted trigonal bipyramidal structure, with imidazole and one peroxo atom in axial position (Figure 2).

Protonation of the anionic cofactor **1** (Chart 1) may, in principle, take place either on oxo or peroxo atoms. In fact, protonation of the peroxo group leads to isomers (not shown) that are less stable by more than 13 kcal mol^{-1} with respect to the corresponding hydroxo species **2**. The inclusion of environment effects, modeled by the COSMO approach,[37] leads to energy differences still larger than 9.5 kcal mol^{-1}. Further protonation of the neutral species **2** might take place either on the axial or equatorial peroxo atoms, as well as on the oxo group (Chart 1 and Figure 2). Protonation of the latter, leading to **3**, is more favored by about 2 kcal mol^{-1} than protonation of the peroxo group (**4** and **5**). The energy of the hydroperoxo isomers **4** and **5** differs by less than 0.3 kcal mol^{-1}. The inclusion of environment effects changes energy differences by less than 1.0 kcal mol^{-1}. These results suggest that the cationic species **3**, **4**, and **5** might coexist at room temperature. Protonation of the peroxo group only slightly affects the O−O distance, which increases by less than 0.04 Å, whereas the bond distance between the protonated peroxo atom and vanadium is more strongly affected (Figure 2).

Chart 1. Schematic Representation of the Different Protonation State of the Cofactor Investigated in the Present Study

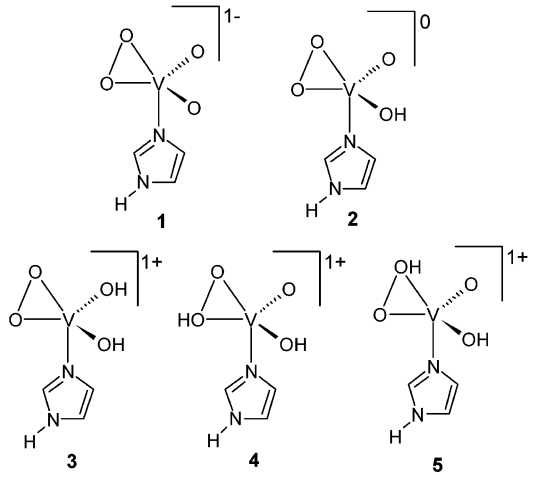

Scheme 1. Schematic Drawing, Not Taking into Account Protonation State, of the Reaction Paths Involving Either Attack to the Axial or Equatorial Oxygen Peroxo Atoms[a]

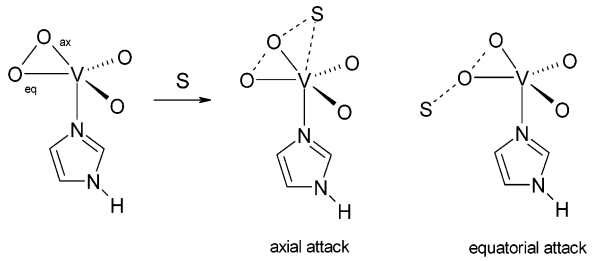

[a] S = Br^- and dimethyl sulfide.

Among the different peroxo species, the structural features of the isomer **2** (Figure 2) are in very good agreement with the X-ray data collected for the peroxo-form of the enzyme (Figure 1),[3] and are consistent with the presence of an unprotonated peroxo, one oxo and one hydroxo group in the vanadium coordination environment.

Reactivity of the Peroxo Forms of the Vanadium Cofactor. Once we had characterized the most stable anionic, neutral, and cationic forms of the peroxo cofactor, we next investigated oxo-transfer reaction pathways involving either the equatorial or the axial peroxo oxygen atom (Scheme 1). Among typical VHPO substrates we have chosen an anionic (Br^-) and a neutral substrate (dimethyl sulfide, hereafter referred to as DMS). It is

(36) (a) Reed, A. E.; Weinstock, R. B.; Weinhold, F. *J. Chem. Phys.* **1985**, *83*, 735; (b) Reed, A. E.; Curtiss, L. A.; Weinhold, F. *Chem. Rev.* **1988**, *88*, 899; (c) Foster, J. P.; Weinhold, F. *J. Am. Chem. Soc.* **1980**, *102*, 7211; (d) Brunk, T. K.; Weinhold, F. *J. Am. Chem. Soc.* **1978**, *101*, 1700; (e) Reed, A. E.; Weinhold, F. *J. Chem. Phys.* **1985**, *83*, 1736; (f) Weinhold, F.; Carpenter, J. E. *The Structure of Small Molecules and Ions*; Plenum 227: New York, 1988.
(37) (a) Klamnt, A. *J. Phys. Chem.* **1995**, *99*, 2224; (b) Klamnt A. *J. Phys. Chem.* **1996**, *100*, 3349.
(38) (a) Warshel, A.; Naray-Szabo, G.; Sussman, F.; Hwang, j.-K. *Biochemistry* **1989**, *28*, 3629; (b) Bottoni, A.; Lanza, C. Z.; Miscione, G. P.; Spinelli D. *J. Am. Chem. Soc.* **2004**, *126*, 1542−1550.

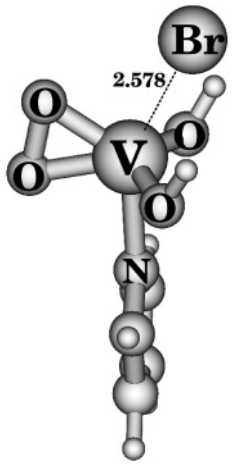

Figure 3. Optimized structures of the van der Waals adduct between Br^- and complex **3** for axial Br^- attack. Relevant distances are in Å.

important to underline that we have chosen two different substrates not to compare their reactivity but to verify that the same general conclusions, related to cofactor reactivity, are obtained independently of substrate choice.

Oxo-transfer involving the equatorial peroxo atom is not compatible with previous coordination of the substrate to the metal center. On the other hand, when considering reaction paths involving the pseudoaxial peroxo atom, one could envision binding of DMS or Br^- to vanadium, followed by oxo-transfer, or direct nucleophilic attack by the substrate on the coordinated peroxide (Scheme 1). To investigate these possibilities, we have optimized structures in which Br^- and DMS occupy the potentially vacant coordination site in **1**−**5**. Even considering the anionic substrate (Br^-) and the cationic forms of the cofactor (**3**, **4**, **5**), the optimized structures are characterized by V−Br or V−S distances larger than 2.5 Å (Figure 3), indicating that weak interaction between the substrate and vanadium takes place prior to the oxo-transfer step.[39]

The reaction paths for the attack of Br^- on both the peroxo oxygen atoms of the anionic species **1** are characterized, even when considering environment effects, by very large potential energy barriers, as expected considering a reaction between two anionic species. When the neutral substrate DMS is considered (**1DMS_a** and **1DMS_e**; Figure 4), the computed potential energy barriers for the attack to the pseudoaxial and equatorial peroxo oxygen atoms are 21.2 and 29.8 kcal mol^{-1}, respectively, which decrease to 14.6 and 18.9 kcal mol^{-1} when taking into account environment effects described by the polarizable continuum medium (see Methods). Remarkably, the oxo-transfer step involving the equatorial peroxo atom evolves to four-coordinated vanadium species due to the cleavage of the V−N bond (not shown), confirming previous evidence indicating that this bond is labilized when an oxo group is trans to the aromatic ring.[29]

Energy barriers computed for the reaction between the anionic substrate Br^- and the neutral species **2** are large in a vacuum (40.6 and 38.0 kcal mol^{-1}, for the attack on axial and equatorial oxygen atoms, respectively), and decrease markedly when considering solvation effects (16.7 and 22.4 kcal mol^{-1}, respectively). The corresponding potential energy barriers for the reaction of **2** with the neutral substrate DMS are 14.8 and 18.2 kcal mol^{-1}, which decrease to 10.0 and 12.4 kcal mol^{-1} considering environment effects. Hence, the oxo-transfer step involving the pseudoaxial peroxo atom is more favored than the corresponding equatorial pathway for both substrates.

The transition state structures (**2Br_a**, **2Br_e**, **2DMS_a**, **2DMS_e**; Figure 4) and the analysis of the imaginary normal modes show that in the oxo transfer step, which resembles a classic SN_2 mechanism, the attack of the nucleophile and the cleavage of the O−O bond are simultaneous. In addition, the angle X−O−O (where X = Br or S) is close to 180°, except for **2Br_a**, where the smaller X−O−O angle is due to weak electrostatic interaction between Br^- and vanadium (Br−V distance = 3.2 Å; Figure 4). The inclusion of environment effects, as simply modeled by the COSMO method, leads always to a reduction of the potential energy barriers with respect to the corresponding value obtained in a vacuum, indicating that transition states are more stabilized than reactants by the polarizable continuum medium. In fact, the heterolytic cleavage of the O−O bond leads to significant charge localization, as deduced by partial charge analysis (not shown). The stabilization of the transition state structure is particularly evident in the case of Br^- oxidation involving the axial peroxo atom (**2Br_a**), where the halide moves away from the metal center going from reactant to transition state, and, therefore, acquires a more pronounced ionic character.

Protonation of **2** leads to the three almost iso-energetic isomers **3**, **4** and **5** (see above) and, therefore, many reaction paths involving the cationic form of the cofactor are conceivable. The computed energy barriers for the reaction of Br^- with the axial and equatorial peroxo atoms of **3** are 20.1 and 20.3 kcal mol^{-1}, respectively (18.8 and 14.7 kcal mol^{-1} considering environment effects), whereas the corresponding values for DMS are 10.9 and 17.0 kcal mol^{-1} (12.3 and 13.8 kcal mol^{-1} considering environment effects).

When considering the hydroperoxo species **4** and **5**, no reaction coordinates corresponding to the attack of the substrates to the protonated peroxo oxygen atom have been found,[40] in agreement with analogous results obtained investigating other hydroperoxo-vanadium complexes.[28] The computed potential energy barriers corresponding to the attack of Br^- and DMS on the axial peroxo atom in **4** (**4Br_a**, **4DMS_a**; Figure 4) are 1.0 and 5.8 kcal mol^{-1}, respectively (3.0 and 5.6 kcal mol^{-1} including solvation effects), whereas the corresponding values computed for the attack on the equatorial oxygen atom of **5** (**5Br_e**, **5DMS_e**; Figure 4) are 6.3 and 13.6 kcal mol^{-1} (6.9 and 9.5 kcal mol^{-1} considering solvation effects). The comparison of the potential energy barriers computed for **3**, **4** and **5** clearly shows that the oxo-transfer step involving the pseudoaxial peroxo atom is markedly more favored than the corresponding equatorial pathway and reveals that the cofactor reactivity is markedly affected by the site at which protonation takes place. In fact, it turns out that the energy barrier for Br^- attack decreases by more than 15 and 7 kcal mol^{-1} going from **3** to the hydroperoxo species **4** and **5**, respectively (Table 1).

(39) Mitchell, A. D.; Cross, L. C. *Table of Interatomic Distances and Configuration in Molecules and Ions*; The Chemical Society, Burlington House: London, 1958; W1.

(40) Such an assertion is supported by the fact that no stationary points corresponding to the previously outlined reaction coordinate have been located. Actually, all the points found by constraining the interatomic distances associated to the reaction coordinate have proven to be multi-saddle points after vibrational analysis; furthermore no negative eigenvalue is associated to an eigenvector representing the reaction coordinate.

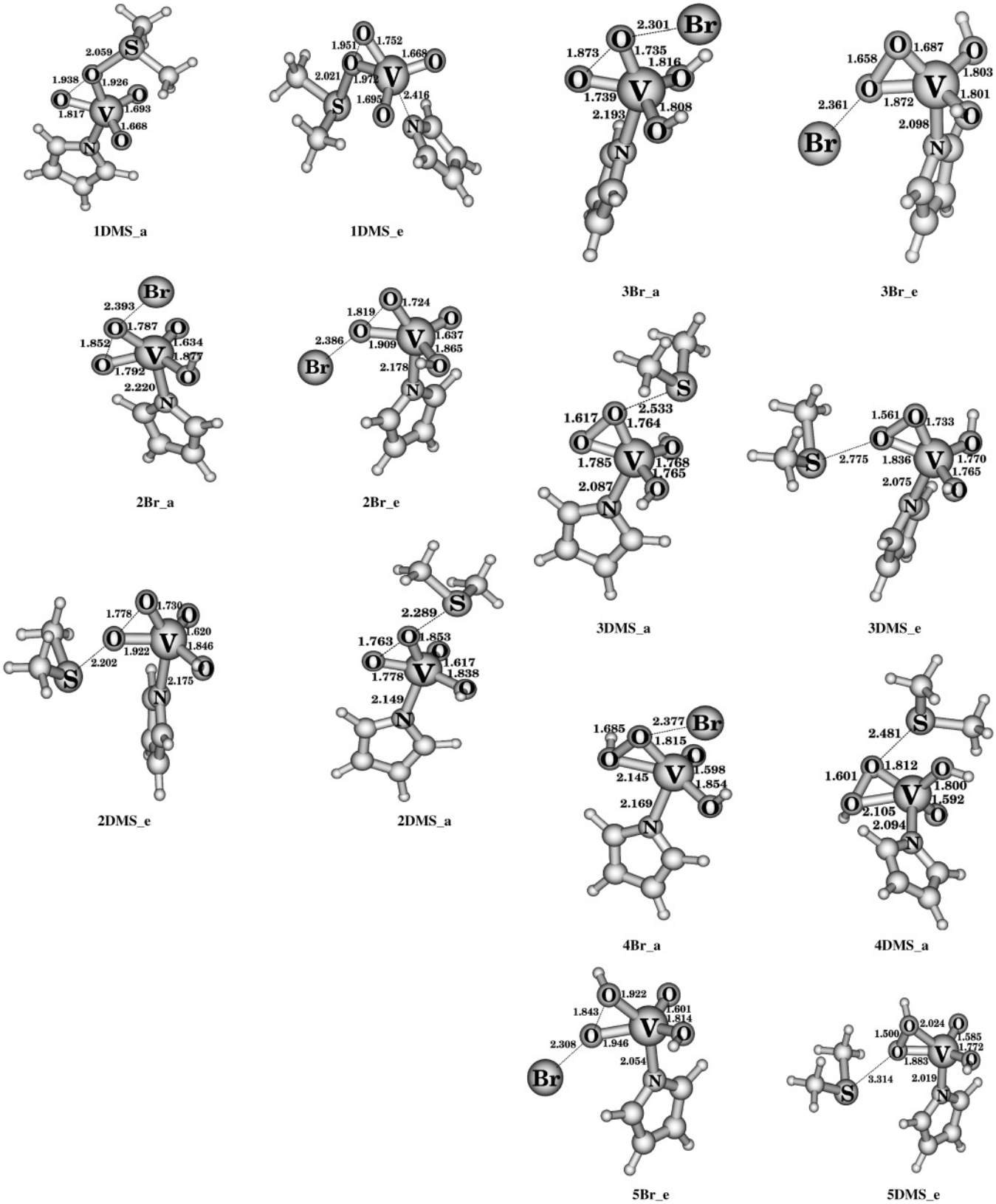

Figure 4. Optimized structures of the transition states. Distances in Å. The alphanumeric code used for labeling the structures is defined as follows: the first character indicates the protonation state of the cofactor according to the nomenclature adopted for the model complexes; the second part defines the substrate of the reaction (either DMS or bromide), whereas the third is related to the reacting peroxo oxygen atom ('a' stands for axial, 'e' for equatorial).

The same trend is observed for DMS, even if the barriers decrease to a lesser extent (Table 2).

An analysis of the electronic properties of of **3**, **4** and **5** helps explaining their different reactivity. The peroxo bond in **3** is very weakly polarized, as deduced by the very similar atomic charges computed for the equatorial (−0.28) and pseudoaxial (−0.30) peroxo atoms. In **4**, protonation of the equatorial peroxo atom leads to a significant polarization of the O−O bond (Δq

Table 1. Potential Energy Barriers (kcal mol^{-1}) for Halide Oxidation[a]

	2 (Br^-)	**3** (Br^-)	**4** (Br^-)	**5** (Br^-)	**6** (Br^-)	**7** (Br^-)	**8** (Br^-)	**6** (Cl^-)	**7** (Cl^-)	**8** (Cl^-)
axial (vacuum)	40.6	20.1	1.0	n.f.	6.7	10.2	11.2	11.3	16.1	14.9
axial (solvent)	16.7	18.8	3.0	n.f.	17.4	n.a.	n.a.	n.a.	n.a.	n.a.
equat. (vacuum)	38.0	20.3	n.f.	6.3	n.a.	n.a.	n.a.	n.a.	n.a.	n.a.
equat. (solvent)	22.4	14.7	n.f.	6.9	n.a.	n.a.	n.a.	n.a.	n.a.	n.a.

[a] The substrate is explicitly indicated in parentheses. The labels n.f. and n.a. stand for 'not found' and 'not available', respectively.

Table 2. Potential Energy Barriers (kcal mol^{-1}) for DMS Oxidation[a]

	1	**2**	**3**	**4**	**5**	**6**
axial (vacuum)	21.2	14.8	10.9	5.8	n. f.	8.5
axial (solvent)	14.6	10.0	12.3	5.6	n.f.	8.9
equat. (vacuum)	29.8	18.2	17.0	n. f.	13.6	n.a.
equat. (solvent)	18.9	12.4	13.8	n.f.	9.5	n.a.

[a] The labels n.f. and n.a. stand for 'not found' and 'not available', respectively.

$= 0.12$), with the pseudoaxial oxygen more electrophilic than the protonated equatorial peroxo atom. Also in **5**, the unprotonated peroxo atom is more electrophilic, but the charge separation becomes smaller ($\Delta q = 0.05$).

Role of Lys353 in the Activation of the Peroxo Moiety. The above results clearly show that the oxo-transfer reaction path involves the unprotonated axial peroxo oxygen atom and highlight the role of protonation of the peroxo moiety in the activation of peroxo-vanadium complexes, in full agreement with experimental data.[9,21] Remarkably, in the peroxide-bound form of the enzyme, a lysine residue (K353) is hydrogen bonded to the equatorial oxygen atom of the peroxo group,[3] which corresponds to the protonated peroxo atom in the more reactive isomer **4**, suggesting that this amino acid might play a role similar to H^+ in peroxide activation. In fact, replacement of K353 with alanine results in a markedly reduced catalytic efficiency, leading to the suggestion that the positively charged residue K353 could polarize the bound peroxide, thus favoring the nucleophilic attack by the substrate.[6] To investigate whether this residue can play a functional role similar to H^+ in promoting peroxo activation, we have studied the oxo-transfer step in a model systems (hereafter referred to as **6**; Figure 5) in which a $CH_3-NH_3^+$ group is hydrogen bonded to the equatorial peroxo oxygen atom of the neutral complex **2**. The potential energy barriers for the reaction **6** + DMS (Figure 5; Table 2) are 8.5 and 8.9 kcal mol^{-1} in a vacuum and considering solvation effects, respectively. Comparison with the corresponding activation barriers computed for **3** and **4** (which have the same overall charge of **6**) indicates that the presence of a polarizing group such as $CH_3-NH_3^+$ plays a role, albeit less dramatic than protonation of the peroxo moiety, in the activation of the peroxo form of the cofactor. In fact, partial atomic charge analysis reveals that the presence of methylammonium causes polarization of the peroxo bond ($\Delta q = 0.07$; Figure 5). It is noteworthy that the substitution of $CH_3NH_3^+$ with an hydrogen bond donor such as CH_3NH_2 or H_2O results in negligible polarization of the peroxo bond and consequent null catalytic effect (not shown). To further verify that the polarization of the peroxo moiety is a key factor for catalysis, we have computed also the transition state for a variant of model **6** (not shown) in which the $CH_3NH_3^+$ group interacts only with the oxo and hydroxo groups of the cofactor. It turns out that the corresponding energy barrier is comparable to that observed for **3** (same overall charge), confirming that the $CH_3NH_3^+$ group lowers the activation barrier only when it interacts with the peroxo group.

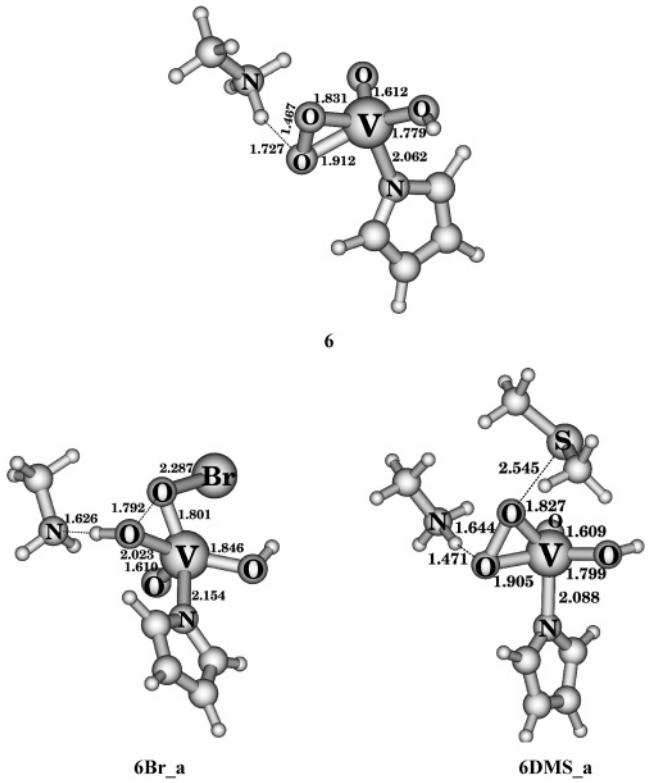

Figure 5. Optimized structures of the model (**6**) in which $CH_3NH_3^+$ is hydrogen bonded to the equatorial peroxo oxygen atom of the neutral cofactor **2**, and corresponding transition state structures for Br^- (**6Br_a**) and DMS (**6DMS_a**) oxidation. Distances in Å.

The presence of a $CH_3NH_3^+$ group interacting with the equatorial peroxo oxygen leads to a very small energy barrier also for Br^- oxidation in a vacuum (6.7 kcal mol^{-1}). However, in this case the inclusion of environment effects has a strong influence on the energy value, leading to a relatively large barrier (17.4 kcal mol^{-1}). The explanation for this result becomes evident once the structure of the transition state for Br^- oxidation is analyzed keeping in mind that energy corrections due to the polarizable continuum medium are computed on molecular structures optimized in a vacuum, following previously reported studies.[37,38] In fact, attempts to carry out geometry optimizations of models systems 'soaked' in the polarizable continuum medium resulted in convergence problems and prohibitive computational times. In the transition state for Br^- oxidation (**6Br_a**; Figure 5) the oxo-transfer is simultaneous to the transfer of a proton from $CH_3-NH_3^+$ to the vanadium cofactor, indicating that the $[ImVO_4HBr]^-$ species formed along the reaction path is sufficiently basic (in a vacuum) to remove a proton from $CH_3-NH_3^+$. This implies that in the oxo-transfer step involving Br^- the reactant is an adduct formed by charged species ($CH_3NH_3^+$, Br^-, $[ImVO_4H]$), while the transition state

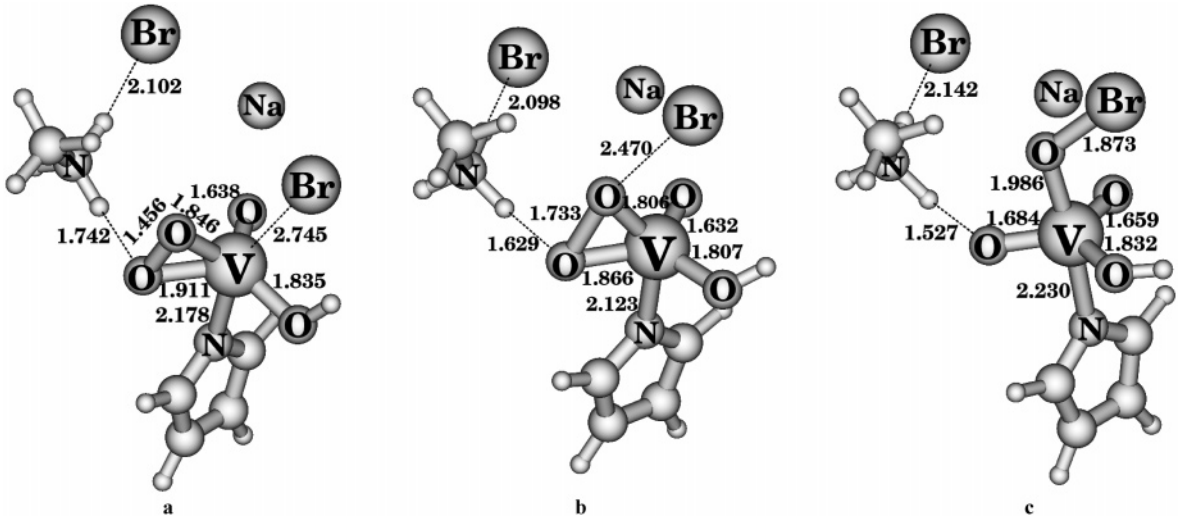

Figure 6. Optimized structures for reactant (**a**), transition state (**b**) and product (**c**) for Br^- oxidation by the model complex **7**. Distances in Å.

is better described as an adduct between two neutral species (CH_3NH_2, $[ImVO_4H_2Br]$; Figure 5). Of course, the zwitterionic reactant is more strongly stabilized than the transition state by the polarizable continuous medium, leading to a large energy barrier.

As a result, the simple description of environment effects by means of energy corrections (by the COSMO approach) computed on structures optimized in a vacuum hampers the answer to relevant questions such as: How can the lysine environment affect the reaction barrier for halide ions? In this context, it is noteworthy that the cofactor environment in the protein active site is characterized by the presence of several positively charged amino acids that could buffer the basicity of the reactants.[3]

To better investigate how the environment can tune the reactivity, we have studied models in which the cofactor environment has been simply described by the presence of counterions, whose presence can be explicitly taken into account during geometry optimization. In the first model (**7**), a Br^- ion has been placed in close proximity to the $CH_3NH_3^+$ group to mimic simply the presence of residues capable of interacting with the lysine side chain. In addition, a Na^+ ion has been placed to interact both with the halide ion and with the neutral cofactor, to mimic the presence of positively charged residues in the cofactor environment (Figure 6). The reactivity of **7** with Br^- and Cl^- has been compared with the reactivity of two other model systems: the first being **6**, which has been described above and where both the lysine model ($CH_3NH_3^+$) and the neutral cofactor are 'unsolvated'; the second (**8**) being a model where a Na^+ is placed in close proximity of the neutral cofactor. All three systems (**6**, **7**, and **8**) have the same overall charge and allow a safe and fair comparison of computed reaction energies.

The optimized structures of reactant, transition state and product for Br^- oxidation by **7** are shown in Figure 6, parts a, b, and c, respectively. Remarkably, proton transfer from CH_3-NH_3^+ to the cofactor is not observed and the potential energy barriers associated with the oxo-transfer step are 10.2 and 16.1 kcal mol^{-1} for Br^- and Cl^-, respectively (Table 1). The overall reactions are exothermic by 7.7 and 1.8 kcal mol^{-1}. It turns out that the corresponding computed potential energy barriers for the reactions involving model **8** are 11.2 and 14.9 kcal mol^{-1}, indicating that the presence of the $R-NH_3^+Br^-$ group slightly decrease the potential energy barrier only for Br^- oxidation.

Scheme 2. Proposed Catalytic Cycle for VHPOs

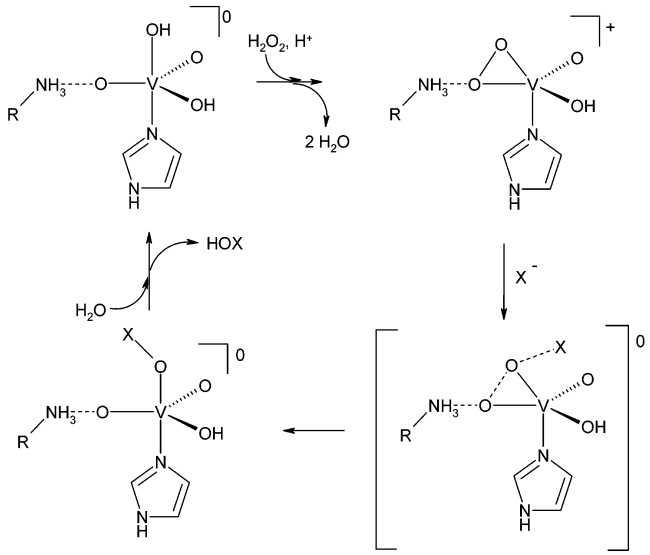

The barriers computed for the reactions **6** + Br^- and **6** + Cl^- are 6.7 (see above) and 11.3 kcal mol^{-1}, respectively. The comparison of results obtained on the two 'limit' models, the first where $R-NH_3^+$, the cofactor and the reacting halide ion are fully unsolvated (**6**; Figure 5), and the second where the ionic character of these group is strongly buffered by counterions (**7**; Figure 6), shows that the environment can markedly tune the reactivity of the metal cofactor. In particular, when the polarizing power of the $R-NH_3^+$ group is drastically reduced by an anionic counterion, its catalytic role is strongly depressed (Br^- oxidation) or fully abolished (Cl^- oxidation). Remarkably, the analysis of the VClPO active site shows that Lys353 does not interact with anionic amino acids,[2,3] is close to a hydrophobic (phenylalanine) residue and is involved in a single hydrogen bond with the backbone carbonyl of a proline residue. On the other hand, in VBrPO the phenylalanine residue is replaced by histidine, which forms an additional hydrogen bond with the lysine residue,[41] buffering its polarizing power. Therefore, on the ground of our results, we propose that this difference is

important to explain the different reactivity of these enzyme families. Besides, these results suggest also that pendant amine functionalities, as present in cleverly designed peroxo-complexes,[30] can play a crucial role in modulating their reactivity properties.

In conclusion, our results elucidate the crucial role of protonation in the activation of the peroxovanadium cofactor. Of most interest, results shed light on the key oxo-transfer step, which implies the attack of the substrate on the *unprotonated pseudoaxial peroxo oxygen atom*. Remarkably, this peroxo oxygen atom is not involved in hydrogen bonding interaction and is easily accessible to substrates in the X-ray structure of the peroxo form of the enzyme.[3] The role of Lys353 in peroxo activation has been also explored, leading to the conclusion that this residue plays its catalytic role by polarizing the peroxo cofactor, in agreement with previous proposals.[6] Moreover, we have shown that the Lys353 environment can significantly affect the catalytic activity, possibly being a crucial factor for tuning the reactivity of the enzyme toward Br^- and Cl^- ions. On the basis of these and previous results[29] a detailed insight into the structural features of key intermediates in the catalytic cycle of VHPO can be proposed (Scheme 2). Further theoretical investigations aimed at characterizing the intimate mechanism of the conversion of the resting to peroxo form of the cofactor, as well as further clarifying the subtle role of the cofactor environment in tuning the polarizing power of Lys353 and promoting the O−O cleavage step, are presently underway.

JA046016X

(41) Weyand, M.; Hecht, H. J.; Kiess, M.; Liaud, M. F.; Vilter, H.; Schomburg, D. *J. Mol. Biol.* **1999**, *293*, 595−611.